ELEMENTA
Science of the Anthropocene

Zavala-Araiza, D, et al. 2018 Methane emissions from oil and gas production sites in Alberta, Canada. *Elem Sci Anth,* 6: 27. DOI: https://doi.org/10.1525/elementa.284

RESEARCH ARTICLE

Methane emissions from oil and gas production sites in Alberta, Canada

Daniel Zavala-Araiza*, Scott C. Herndon†, Joseph R. Roscioli†, Tara I. Yacovitch†, Matthew R. Johnson‡, David R. Tyner‡, Mark Omara* and Berk Knighton§

We performed ground-based measurements (downwind, site-wide characterization) of methane emissions from older light oil and natural gas production sites in Alberta, Canada (Red Deer region, 60 measured sites). We developed a distribution of site-based methane emissions and as previously found in production regions in the United States, a small fraction of the sites account for the majority of methane emissions: 20% of the sites emit three quarters of the methane from oil and gas production. Using empirically derived emission factors, we compared an estimate of regional methane emissions, to a top-down airborne-based measurement of the same region. The airborne measurement was 35% lower, though not statistically different (4,800 ± 3,200 vs. 3,100 ± 2,200 kg CH_4 h^{-1}). In Alberta, the majority of these oil and gas emissions go unreported under current reporting requirements. Effective mitigation will most likely require frequent monitoring to identify high-emitting sites as well as leaky components that we hypothesize are also a major contributor to emissions.

Keywords: methane; greenhouse gases; fossil fuels; oil and gas industry; Canada; downwind measurements

Introduction

Mitigating methane (CH_4) emissions from the global oil and gas system represents a major opportunity to reduce the near-term climatic effects of this powerful greenhouse gas (GHG) (Bousquet et al., 2006; Shoemaker et al., 2013; Saunois et al., 2016; Höglund-Isaksson, 2017). Several countries have announced pledges to reduce CH_4 emissions from this system (Mexico: Presidencia de la Republica, 2016; Climate & Clean Air Coalition, 2016; Environment and Climate Change Canada, 2017a), with Canada and the US taking concrete steps to regulate emissions (US EPA, 2016; Environment and Climate Change Canada, 2017b).

In Canada, the oil and gas system is the major anthropogenic source of CH_4 emissions, accounting for almost half of total CH_4 emissions in the inventory (Environment and Climate Change Canada, 2016). The Canadian government recently announced regulations that support the goal of a 40–45% reduction of CH_4 emissions from the oil and gas system below 2012 levels by the year 2025 (Environment and Climate Change Canada, 2017b). Similarly, Alberta — the largest fossil fuel producing province in Canada — announced a 45% reduction goal and is developing its own set of regulations (Alberta Government, 2016). For federal and provincial goals to be realistically achieved and for the regulations to work, we need to know the current emissions baseline as well as the characteristics of the major emitting sources (e.g., spatial and temporal patterns, emissions distributions).

An extensive body of research has successfully reduced the uncertainty in terms of CH_4 emissions from the US oil and gas system (Allen et al., 2013; Allen, Pacsi, et al., 2015; Allen, Sullivan, et al., 2015; Lamb et al., 2015; Mitchell et al., 2015; Zimmerle et al., 2015; Omara et al., 2016). Relevant lessons include (i) identification of major emission sources across the natural gas supply chain (Allen, Pacsi, et al., 2015; Allen, Sullivan, et al., 2015; Lamb et al., 2015; Zimmerle et al., 2015; Marchese et al., 2015), (ii) proof that high-emitting sources disproportionately account for the majority of emissions (Brandt et al., 2014; Zavala-Araiza, Lyon, et al., 2015; Brandt et al., 2016; Omara et al., 2016; Lyon et al., 2016; Zavala-Araiza et al., 2017), and (iii) examples of smart regulations significantly reducing emissions from different sources (e.g., green completions, replacement of high-emitting pneumatic controllers) (Allen et al., 2013; Allen, Pacsi, et al., 2015). With a limited number of studies reporting empirical observations of oil and gas methane emissions outside the US — and specifically in Canada — (Johnson et al., 2017; Atherton et al., 2017) the question remains about whether the same emission characteristics found in the US apply elsewhere.

* Environmental Defense Fund, Austin, Texas, US
† Aerodyne Research Inc., Billerica, Massachusetts, US
‡ Energy and Emissions Research Laboratory, Department of Mechanical and Aerospace Engineering, Carleton University, Ottawa, Ontario, K1S 5B6, CA
§ Department of Chemistry and Biochemistry, Montana State University, Bozeman, Montana, US
Corresponding author: Daniel Zavala-Araiza (dzavala@edf.org)

The main motivation behind the empirical data collected and analyzed here is to compare the emission patterns from oil and gas production sites of Alberta, Canada, to previously reported datasets of emissions from the US. If we were to find similarities, it would be possible to translate the multiple lessons learned in the US in terms of improving emission inventories, reducing emissions, and establishing effective and efficient regulations.

In this work, we (i) present empirical site-level estimates of CH_4 emissions from oil and gas production sites in Alberta derived from downwind ground-based measurements, (ii) characterize the emissions distribution and discuss its implications, and (iii) re-analyze five additional datasets to present a systematic and consistent comparison of CH_4 emissions from production sites across seven production basins in North America. As described below, we report measurements of production sites near Red Deer, Alberta — a region characterized by older natural gas production sites and light oil production (i.e., average age 15 years; age range: 0.8–55 years) (i.e., average gas production per site: 98 thousand cubic feet per day (Mcf d^{-1}), average oil production per site: 3.4 barrels per day (bbl d^{-1})).

Methods

Sampling strategy

The quantification of site-level CH_4 emissions took place using an instrumented mobile laboratory. During the first week of November 2016, the miniature Aerodyne Mobile Laboratory (minAML) performed measurements in the oil and gas production region near Red Deer, Alberta (**Figure 1**). The Alberta Energy Regulator (AER) provided site access, which allowed quasi-random site selection (constrained by wind and road conditions) by the sampling team. Prior to the start of the measurements, the sampling team had a spatially-explicit list of active production sites. The list of wells was based on publicly available data from AER, (Alberta Energy Regulator, 2017) and then clustered into production sites as described in Zavala-Araiza et al. (Zavala-Araiza, Lyon, et al., 2015). Data on production site characteristics (e.g., age, gas production, oil production) were obtained from Drillinginfo (DI Desktop, 2017).

The research team conducted two types of experiments to quantify CH_4 emission rates of specific facilities. In the first, a method using controlled releases of tracer gas was employed (tracer flux method, hereafter). The second approach used an atmospheric dispersion algorithm to estimate CH_4 emissions from sites where the tracer release was not conducted (Gaussian dispersion method, hereafter). To deploy these two approaches, the sampling team randomly selected suitable sites for the tracer flux method, and in transit between tracer measurements would capture plume data suitable for posterior analysis using the Gaussian dispersion method. These fortuitous plume measurements have a higher probability of capturing bigger plumes related to sites with higher emissions, and do not capture sites with no emissions. As a consequence, we can characterize the tracer flux sample as a systematic sample, and the Gaussian dispersion sample as biased towards higher emissions (see discussion below).

The details of the deployment platform, the analytical equipment, and the two measurement approaches are briefly summarized below, with more details provided in SM, Text S1, Section 1.

Mobile laboratory

The minAML acted as the deployment platform for the meteorological, GPS and analytical equipment used in these measurements. The design, and operational and analysis protocols used in the minAML are inherited from the Aerodyne Mobile Laboratory deployments (Kolb et al., 2004; Herndon et al., 2005; Roscioli et al., 2015). For this deployment, ambient air was continuously analyzed for CH_4, ethane (C_2H_6), and tracer release gases as well as other trace gas species. A modified pickup truck that

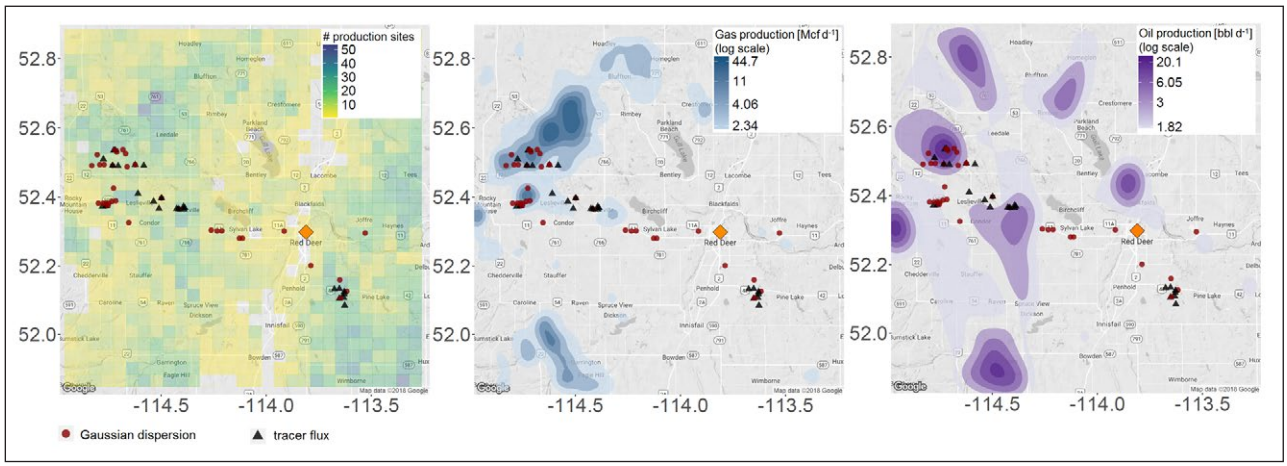

Figure 1: Maps illustrating the location of measured oil and gas production sites. Measurements using the tracer flux method are shown as black triangles (N = 25) while measurements using Gaussian dispersion method are shown as red dots (N = 35). Left: density of production sites. Middle and right: contour plots illustrating hotspots of gas production and oil production, respectively. All measurements were performed within an 80 km radius of Red Deer. The area shown in the maps includes a total of 11,000 production sites (12,600 wells) with a site mean gas production of 98 Mcf d^{-1} (2.8 × 1000 m^3 d^{-1}) and site mean oil production of 3.4 bbl d^{-1} (0.54 m^3 d^{-1}). DOI: https://doi.org/10.1525/elementa.284.f1

accompanied the minAML also quantified meteorological parameters and is referred to as the tracer release vehicle.

An AirMar 200WX anemometer mounted on the sample mast was used to measure wind speed and direction. The position and heading of the minAML was determined by a Hemisphere GPS model V100.

The sample inlet was 2.2 m above ground, on the passenger side, and extended to the front bumper of the vehicle. Ambient air was continuously sampled through a ½" outer diameter (O.D.) Teflon tube. Three flow paths diverge, with 625 standard cubic centimeters per minute (sccm) splitting out to a LiCor-6262A (CO_2), ~500 sccm are directed to a Proton Transfer Reaction Mass Spectrometer (PTRMS) (Knighton et al., 2012) and 6000 sccm to the three infrared laser spectrometers in series (McManus et al., 2015). An upstream pressure controller regulated the cell pressure in the tunable infrared laser spectrometers. The typical mobile laboratory operating protocols and sampling techniques have been described previously (Herndon et al., 2005; Yacovitch et al., 2017).

Three tunable infrared direct absorption spectrometers (TILDAS) quantified nitrous oxide (N_2O), CH_4, C_2H_6, and propane (C_3H_8) as well as carbon monoxide (CO) and water vapor (H_2O) (McManus et al., 2015). A thorough description of the TILDAS instruments is documented elsewhere (McManus et al., 2015), but some brief details of how they were deployed on this project are warranted. The first spectrometer quantified N_2O, H_2O and CH_4 using the rotation-vibration absorption lines between 1300.8 and 1301.7 cm^{-1}. The second spectrometer was outfitted with two lasers, with the first quantifying CH_4 and C_2H_6 using the lines at 2990 cm^{-1}, and C_3H_8 at 2965 cm^{-1}. The final laser spectrometer measured N_2O, CO and H_2O at 2200 cm^{-1}. Note that there were redundant measurements of CH_4, N_2O and H_2O. Further details of the TILDAS instruments are documented elsewhere (Yacovitch et al., 2014).

Calibrations of the CH_4 mixing ratio were performed using a compressed gas cylinder containing 777 ± 7.8 ppmv CH_4 (1%). Calibrations of the N_2O tracer were performed before and after the measurement project using the procedure described in the supplemental information section. Propagation of uncertainties in the calibration factors suggested that the systematic uncertainty in the molar ratio of CH_4/N_2O was 1.8%.

Tracer flux method

The measurement experiment consisted of driving the tracer release vehicle to a well-site and beginning the steady release of a controlled flow of pure gas. N_2O tracer gas was released using an Alicat Flow Controller (MCR-20). Calibration verification was performed up to 20 SLPM. At the flow rates used in this work, we assessed the systematic uncertainty in the N_2O release rate to be 1.02%. The purity stated by the manufacturer (Praxair) was 99.2%.

The minAML conducted 4 to 20 transects of the tracer plume downwind (typically 50–1500 m). The sites were selected strictly on the basis of wind direction and suitable downwind roadways as well as road access to the well pad for the tracer release vehicle. One of the measurement days during the campaign was done without site access and the tracer release was limited to safe parking locations on public roads.

The tracer flux quantification method involves releasing a controlled amount of tracer gas(es) close to likely sources at the site (Lamb et al., 1995; Roscioli et al., 2015). Geographically resolved transects of the emission gas (e.g., CH_4 and C_2H_6) and tracer could then be measured downwind. Unlike other downwind quantification techniques (Brantley et al., 2014; US EPA, 2014; Yacovitch et al., 2015), the tracer flux method requires no knowledge or simulation of atmospheric dispersion. While wind is measured on-site and on the minAML, this information is only used as a diagnostic to direct where the tracer plume should be sought. The downwind measurement transects are used to probe how the enhancements above background for both the tracer species and emitted CH_4 are spatially coherent. This is a critical data quality indicator for the tracer flux method. Coupled with the measurement of the C_2H_6/CH_4 enhancement ratio, these spatial characteristics of the downwind transects allow attribution of the observed CH_4 emissions to the site. Interfering sources of CH_4 are identified due to the lack of coherence with the tracer gas and are not quantified by the tracer flux method.

For each well pad, the minAML collected a sequence of downwind plume transects (**Figure 2**). When the data exhibit the extent of correlation shown in this figure, the molar ratio of CH_4 and tracer species determines the CH_4 emission rate together with the known tracer flow rate (Equation 1).

$$CH_4\ emission\left[kg\ h^{-1}\right] = N_2O\ flow\left[kg\ h^{-1}\right] \times \frac{CH_4\ measured\ [ppb]}{N_2O\ measured\ [ppb]} \quad \text{(Eq. 1)}$$

When the data do not exhibit spatial correlation like the data in **Figure 2**, the area under the CH_4 and tracer plumes are used to determine the molar ratio. An automated algorithm chose the best analysis approach based on R^2 values for the linear fits of mixing ratio correlation. Thorough descriptions of the analysis protocol and the method choice algorithm is discussed elsewhere (Roscioli et al., 2015). The site-representative CH_4 emission rate was computed as the arithmetic mean of all quantified plumes and uncertainty estimated based on the statistical characterizations of the sampled population (Roscioli et al., 2015).

Gaussian dispersion method

The experimental data used in these simulations consisted of periods of data, typically 1–5 min, taken in motion, and showing the CH_4 mixing ratio rise above then return to nominal background value. In this technique, the entire cross-section of a plume is transected at a single height, which differs from other methods using sensor array networks or stationary sampling at a single point combined with measurements of wind fluctuations (Thoma et al., 2012; Brantley et al., 2014).

The dispersion modeling described below is based on the standard Gaussian dispersion equations and procedures (Turner, 1994). Equation 2 relates the measured concentration of emissions (C) at a position × meters

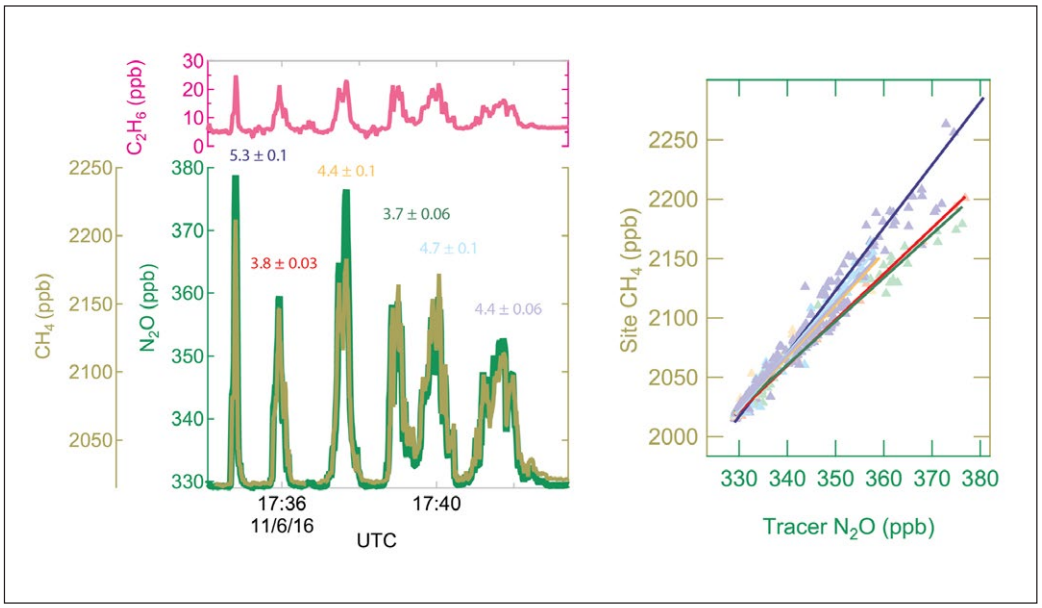

Figure 2: Sample of the time series with multiple plume transects collected with the tracer flux method. Measured mixing ratios (left) of C_2H_6 (pink) CH_4 (dark yellow) and N_2O (green) show correlated increases during each site transect. A time-aligned correlation plot (right) of CH_4 vs N_2O shows the linear fits (molar ratios) used for quantification (each individual site transect colored differently). Range of molar ratios shown in the plot is 3.7 ± 0.06 (R^2 = 0.97) to 5.3 ± 0.1 (R^2 = 0.98); with a mean of 4.4 ± 0.6 (1-sigma uncertainty). Nominal flow rate of N_2O (tracer) = 10 SLPM @ T = 298 K. Emission rate for the site shown in this figure = 1.7 kg CH_4 h^{-1} (1.6–1.9 kg CH_4 h^{-1}). DOI: https://doi.org/10.1525/elementa.284.f2

downwind, y meters off-axis, and z_r meters above ground. The source emission rate (Q), the horizontal wind velocity (u) and the height above ground of the plume centerline (H_e) are required, along with terms for vertical (σ_z) and horizontal (σ_y) dispersion. These dispersion terms are taken from a lookup table based on a chosen Pasquill stability class and are a function of ×, the downwind distance (see Text S1 for detailed description of input parameters as well as an estimation of error).

$$C = \frac{Q}{u\sigma_z\sigma_y 2\pi} e^{-y^2/2\sigma_y^2}\left(e^{-(z_r-H_e)^2/2\sigma_z^2} + e^{-(z_r+H_e)^2/2\sigma_z^2}\right) \quad \text{(Eq. 2)}$$

In practice, the concentrations are computed using a fixed emission magnitude (Q = 1 g/s), and the simulated plume scaled to the experimentally observed mixing ratios. This same scaling factor is applied to Q, yielding the final emission magnitude determination (see example in **Figure 3**). Source location is an important component of these simulations and is discussed in detail in Text S1.

Characterization of the site-level emissions distribution and derivation of emission factors

We derived an emissions probability density function (pdf) that characterizes the production sites measured during this study using the statistical estimator developed by Zavala-Araiza et al. (Zavala-Araiza, Lyon, et al., 2015). This estimator allowed the integration of a systematic sample and a high-emitter biased sample to derive a facility-wide pdf representative of an entire population of sites (see SM, Text S1, Section 2 for description of the statistical estimator).

In addition to deriving the pdf, we also: (i) explored the relationship between emissions and production site parameters (i.e., oil/gas production, age of wells), (ii) compared measured emissions with reported emissions, and (iii) compared emissions in the Red Deer region with the emissions from other production regions in North America. To complete this final task, we re-analyzed five additional datasets to present a systematic and consistent comparison of CH_4 emissions from production sites across seven production basins in North America. Our analysis produces probability emission distributions, which are needed to assess the presence and effect of super-emitters (i.e., sites with excess of emissions related to abnormal process conditions) (Zavala-Araiza et al., 2017).

Results and discussion

Characterization of collected data

We performed a total of 60 measurements: 25 using the tracer flux method and 35 using the Gaussian dispersion method (see File S1 for dataset of measurements and Table S2). Four sites were measured by both methods, but measurements occurred at different times, thus they are considered independent samples. **Figure 4** illustrates the distribution of measurements from both methods. The measurements from the Gaussian dispersion method are shifted towards higher emission rates (mean for the tracer flux method is 2.0 kg CH_4 h^{-1} and 8.0 kg CH_4 h^{-1} for the Gaussian dispersion method). As previously mentioned, this is expected because the tracer flux method

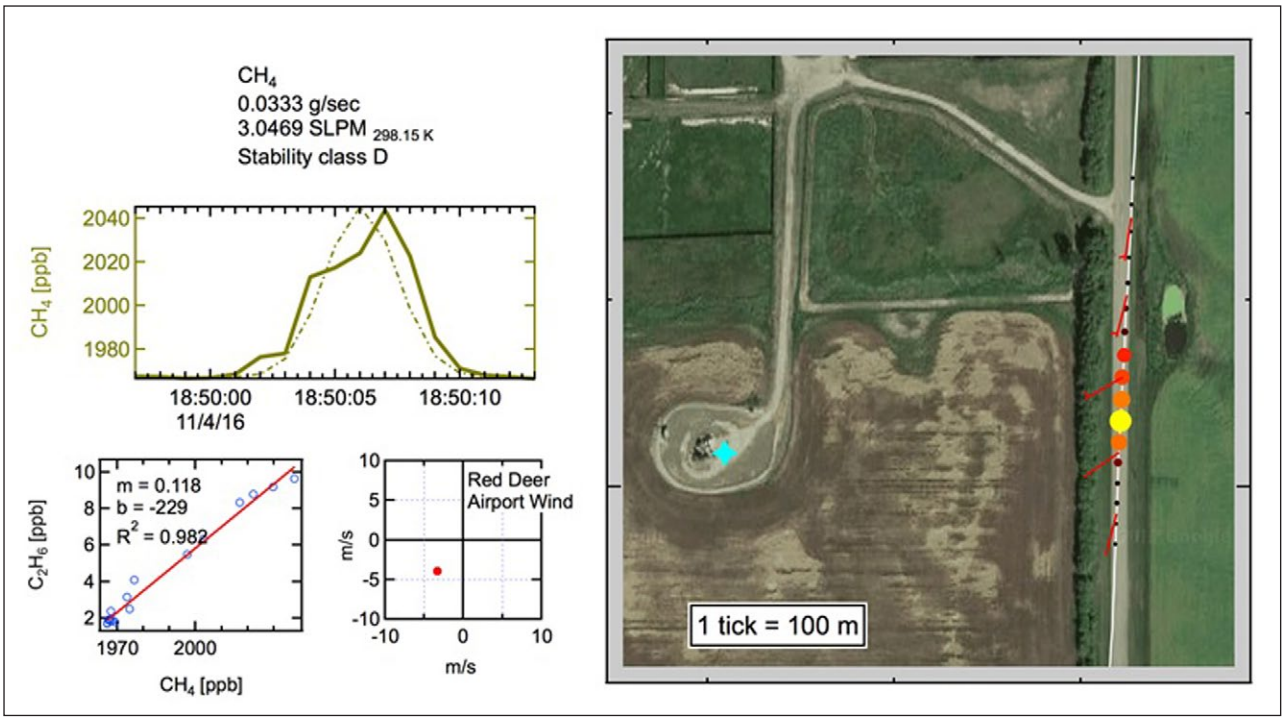

Figure 3: Example of a production site measured with the Gaussian dispersion method. Measured (solid dark yellow trace) and simulated (dotted trace) mixing ratios of CH_4 are shown (top left) along with this data's C_2H_6/CH_4 ratio (bottom left, ratio of 11.8%). Southwest wind measured at a nearby airport is shown (bottom center graph). A site map (right) shows the driven path (circle markers) with markers colored and sized by CH_4 enhancement (small black circles for lowest concentrations, larger red, orange and yellow circles for CH_4 enhancements). The chosen point-source for the simulation is shown (blue star). Wind barbs (red arrows) point towards the site and agree with nearby airport wind (bottom center). DOI: https://doi.org/10.1525/elementa.284.f3

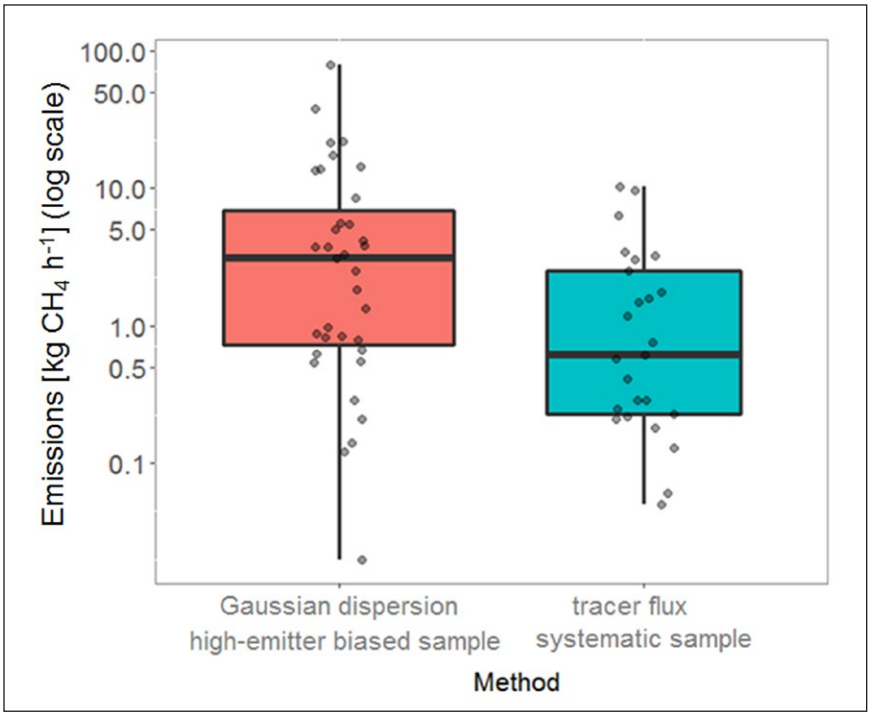

Figure 4: Distribution of measured emission rates under each measurement method. The horizontal line at the middle of each box represents the median; the vertical bounds of the boxes show the 25th and 75th percentiles. The width of the boxes represents the relative sample size for each method. The maximum and minimum values are represented by the length of the whiskers. The data points (with jitter) are overlaid on top of the boxplots. Total measured emissions from systematic sample: 49 kg CH_4 h^{-1} and for the high-emitter biased sample: 280 kg CH_4 h^{-1}. DOI: https://doi.org/10.1525/elementa.284.f4

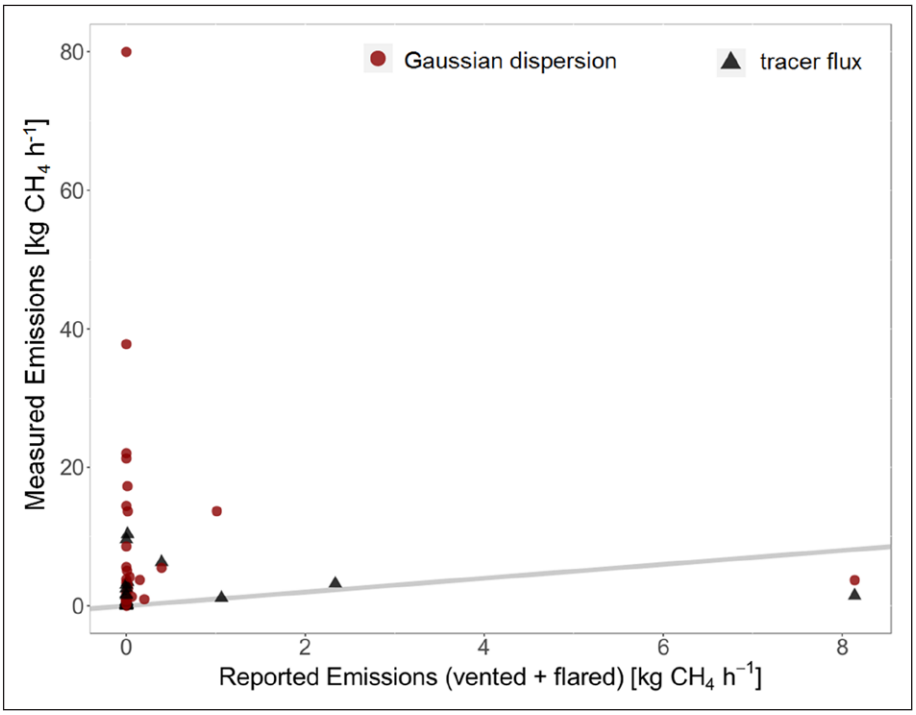

Figure 5: Comparison of measured emissions with reported emissions. Triangles represent sites where the tracer flux method (systematic sample) was used, and red circles represent sites where the Gaussian dispersion method (high-emitter biased sample) was used. The grey line represents a 1:1 relationship between measured and reported emissions. Please note the different x- and y-axis scales. DOI: https://doi.org/10.1525/elementa.284.f5

is capturing a systematic sample of the population while the Gaussian dispersion method is biased towards bigger plumes (higher emitters). Hereafter we will refer to the tracer flux method sample as the systematic sample, and the Gaussian dispersion method sample as the high-emitter biased sample.

In line with previous studies in the US (Brantley et al., 2014; Lan et al., 2015; Rella et al., 2015; Yacovitch et al., 2015; Zavala-Araiza, Lyon, et al., 2015; Omara et al., 2016; Robertson et al., 2017), our measurements are characterized by skewed distributions: for the systematic sample 20% (5 of 25) of the measurements account for 68% (33 of 49 kg CH_4 h^{-1}) of total measured emissions, while for the high-emitter biased sample 29% (10 of 35) of the measurements account for 85% of total measured emissions (240 of 280 kg CH_4 h^{-1}).

Major sources of emissions are mainly unreported

For every measured production site, we evaluated the reported emissions during the month of the study, based on vented and flared whole gas volumes reported by industry under AER's Directive 60 (AER, 2016). Reported vented volumes "(...) are assumed to comprise, where applicable, casing gas venting, waste associated gas flows, treater and stabilizer off-gas and gas volumes discharged during process upsets and equipment depressurization events (i.e., blowdowns)." (Clearstone Engineering Ltd., 2014). CH_4 emissions from these reported volumes were calculated as in Johnson et al. (Johnson et al., 2017) using site specific gas composition estimates derived using an AER data set of 310,000 useable gas samples associated with 120,000 well segments located throughout the province. Flare efficiencies were assumed to be 98%. Venting accounted for the dominant majority (98%) of the CH_4 emissions associated with reported gas volumes (reported emissions per site are included in File S1). Six sites classified as active had no reported production (oil or gas) during the month of the study, but they still had emissions ranging between 0.21 kg CH_4 h^{-1} to 38 kg CH_4 h^{-1}.

Total measured emissions were 15 times higher than total reported emissions (330 kg CH_4 h^{-1} vs. 22 kg CH_4 h^{-1}), and 60% of the measured sites reported zero emissions but emissions were detectable (**Figure 5**). These results highlight that the majority of the emissions in the Red Deer region are related to currently unreported sources, such as equipment leaks, emissions from pneumatic controllers, and unreported venting.

Multiple regression analysis

We used the systematic sample to perform a multiple regression analysis and explore the relationship between emissions and several production parameters at each site (i.e., gas production, oil production, age of wells, well type, and number of wells per site).

In our final regression model, emissions are a function of oil production, gas production, age, and an interaction term between age and gas production. This model explains roughly two-thirds of the variance in CH_4 emissions (R^2_{adj} = 0.640, $p < 1 \times 10^{-4}$). Of the explained variance, gas production is responsible for 80% of the variance, the interaction term for 13%, oil production 5.0% and age 2.0% (SM, Text S1, Section 4).

The interaction term in the model (gas production and age) underscores how emissions as a function of gas production increase differently as a site gets older. We see a higher increase in emissions as we transition to older

sites (SM, Text S1, Figure S-3). This could be explained by the fact that older sites are more prone to situations that could cause excess emissions (e.g., malfunctions, or failures from older equipment). If any of these issues manifest at an old site, higher gas production translates into a higher volume of gas that could potentially be released to the atmosphere. It is expected that for any given site, gas production will decrease as a function of age (Baihly et al., 2010; Zavala-Araiza, Allen, et al., 2015). Nonetheless, the interaction term in our model captures the aggregate effect of the population of sites where we observe a significant number of older sites (age > 30 years) with substantial gas production (>150 Mcf d^{-1}).

On top of the relationship between age, gas production and emissions, our model suggests that oil producing sites tend to have higher emissions than sites without oil production: higher emissions are expected at sites with higher oil production (e.g., venting from condensate tanks (Lyon et al., 2016; Lavoie et al., 2017)).

Even though the explained variance is high enough to consider the relationships relevant, we acknowledge that it is still low in terms of appropriate predictive power. We hypothesize that the other one-third of unexplained variance in CH_4 emissions could be related to abnormal process conditions that have been reported in previous studies and would escape the routine behavior characterized by production levels and age (Zavala-Araiza et al., 2017). For example, Mitchell et al. (Mitchell et al., 2015) reported measurements of natural gas gathering and processing facilities in the US and as part of their analysis they tested similar regression models to the one that we present here. In addition, through a partnership with the operators, they were able to identify high-emission episodes at some of the measured facilities. The predictive power of their model increased in a statistically significant way when a categorical variable was included for those sites that were flagged as sites with abnormal process conditions (e.g., substantial venting).

Emissions distribution: disproportionate impact of high-emitting sites

Using two variations of the statistical estimator we derived pdfs that follow lognormal distributions:

(i) Using the systematic samples only; which relies on a measurement method with lower uncertainties but uses a small sample size (N = 25, μ = –0.31 σ = 1.5).

(ii) Integrating the systematic sample and the high-emitter biased sample into a single distribution; which allows us to assess the impact of the low probability, high emitters that have emissions greater than the systematic sample maxima (N = 60, μ = –0.31 σ = 1.7).

The emission factors (EF) that characterize production sites in the region are 2.2 kg CH_4 h^{-1} (95% confidence interval [CI]: 1.0, 5.4 kg CH_4 h^{-1}) for (i), and 2.9 kg CH_4 h^{-1} (CI: 1.3, 6.8 kg CH_4 h^{-1}) for (ii) (see SM, Text S1, Section 2 for discussions about the difference between EFs and the statistical estimator.)

Plots in **Figure 6** illustrate the disproportionate contribution of high-emitting sites to total emissions. While 50% of the sites with lower emissions only contribute 4–7% of total emissions, the 20% of sites with highest emissions contributes 74–79% of total emissions. Similarly, the 10% of sites with highest emissions is responsible for 58–65% of total emissions. In terms of absolute emission rates, 9.7–22% of sites have emissions greater than 5.0 kg CH_4 h^{-1}, and 3.9–12% of sites have emissions in excess of 10 kg CH_4 h^{-1}.

Using a bootstrap analysis (Efron and Tibshirani, 1993), we draw a random mean from the distribution of each of

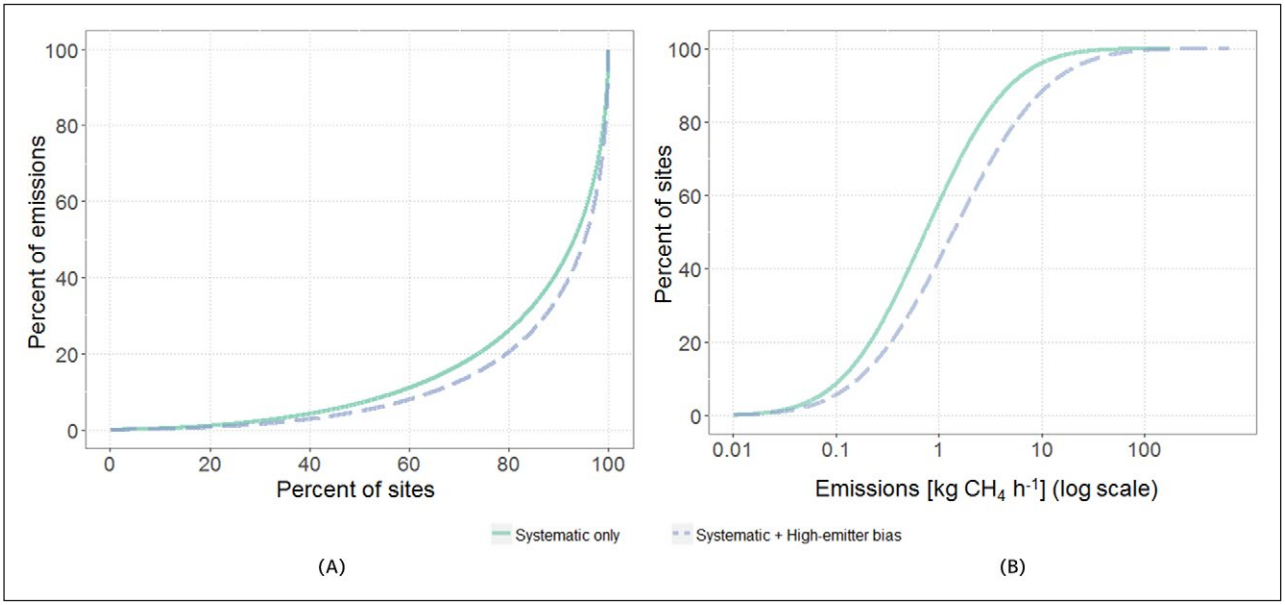

Figure 6: (A) Lorenz curve: percent of emissions as a function of percent of sites. **(B)** Cumulative distribution functions. Both panels show the pdfs derived under both statistical estimator variations: systematic samples only (green) and integrating systematic samples with the high-emitter biased samples (blue, dashed line). DOI: https://doi.org/10.1525/elementa.284.f6

the two generated EFs with their associated confidence interval (assuming Gaussian distribution), leading to a central estimate of 2.6 kg CH_4 h^{-1} (CI: 0.84, 4.3 kg CH_4 h^{-1}). We use this central estimate to characterize regional emissions.

Johnson et al. report a top-down regional airborne-based estimate of CH_4 emissions from oil and gas operations in a 50 km by 50 km box in the Red Deer region (SM, Text S1, Section S5 and Figure S-4) of 3,100 kg CH_4 h^{-1} (CI: 900; 5,300 kg CH_4 h^{-1}) (Johnson et al., 2017). Even though only 40% of the ground-based measurements are inside the source region surveyed by the aircraft, the flight boundaries were selected to be representative of the activity in the Red Deer region which is dominated by upstream gas and oil production sites. If we use our central estimate to extrapolate emissions for the entire box (which contained 1,845 production sites), total emissions are 4,800 kg CH_4 h^{-1} (CI: 1,500; 7,900 kg CH_4 h^{-1}). Thus, the ground-based estimate and the airborne-based estimate agree within confidence intervals.

Analysis of proportional loss rates

The proportional loss rate (CH_4 emissions normalized by CH_4 production) is another commonly used metric to characterize emissions from natural gas production sites (Mitchell et al., 2015; Zavala-Araiza, Lyon, et al., 2015; Omara et al., 2016; Robertson et al., 2017). This metric can simplify the intercomparison among production regions with similar characteristics (e.g., similar gas/oil production volumes). In addition, it can sometimes be an effective way to identify sites that have an excess of emissions related to abnormal process conditions (e.g., malfunctions or equipment issues) (Zavala-Araiza, Lyon, et al., 2015; Zavala-Araiza et al., 2017).

We also replicated the analysis performed in Zavala-Araiza et al. (Zavala-Araiza, Lyon, et al., 2015); where we generated the joint density between emissions and production to estimate the pdf of proportional loss rates (**Figure 7**, and SM, Text S1, Section 6). From this analysis we find that 82% of sites emit >1% of their production, and they are responsible for 91% of the emissions. Similarly, 21% of sites emit >10% of their CH_4 production, accounting for 35% of emissions. Half the sites have proportional loss rate >3.3% and they account for 67% of emissions. It is important to note that the distribution of loss rates is skewed. Although the loss rates are potentially high, this is largely an effect of the small gas production volumes at most sites in the region. Thus, one needs to be cautious in directly comparing the loss rates in the Red Deer region to those observed in other regions with different production characteristics (and in particular, those with lower ratios of oil to gas wells).

Comparison between oil and gas production sites from different production regions of North America

To contextualize the Red Deer emissions distribution, we compared our results with several US oil and gas production regions where similar ground-based measurements of production sites have been performed. In this analysis we include the measurements reported for: Barnett Shale, Texas (Rella et al., 2015; Zavala-Araiza, Lyon, et al., 2015); Denver-Julesburg, Colorado (Brantley et al., 2014; Robertson et al., 2017); Fayetteville, Arkansas (Robertson et al., 2017); Marcellus Shale, Pennsylvania and West Virginia (Omara et al., 2016); Uintah, Utah (Robertson et al., 2017); and Upper Green River; Wyoming (Robertson et al., 2017).

With the exception of the Barnett Shale dataset— for which the statistical estimator approach was originally developed and applied— different estimation methods were used to derive EFs and characterize the other basins. To consistently compare the emission profiles, we took the site-level measurements for each region and replicated the statistical estimator approach (SM, Text S1, Section 7, Table S-4).

Figure 8 shows the pdf of each production region. In all cases we find skewed distributions. Previous work has looked at the presence of high-emitting sites across different producing regions in the US (Lyon et al., 2016), highlighting their dynamic behavior (in space and time) as well as their unpredictability. While a combination of production characteristics and operation practices could

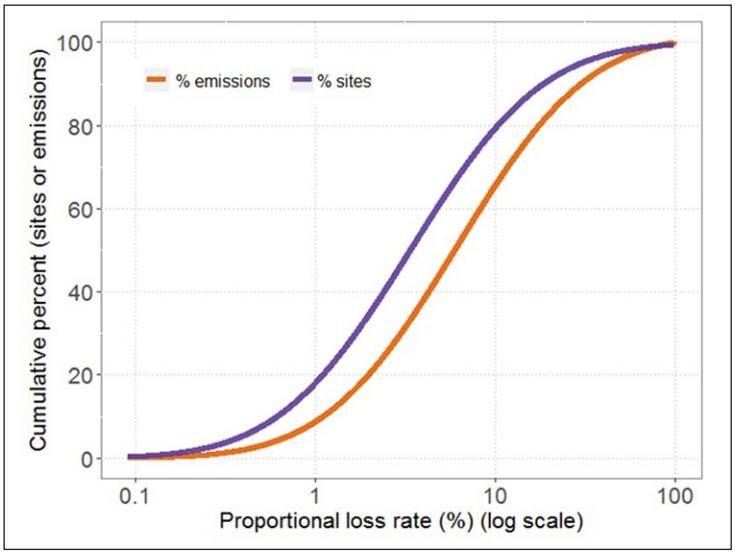

Figure 7: Cumulative percent of sites (purple line) and cumulative percent of emissions (orange line) as a function of proportional loss rates (emissions normalized by CH_4 production). DOI: https://doi.org/10.1525/elementa.284.f7

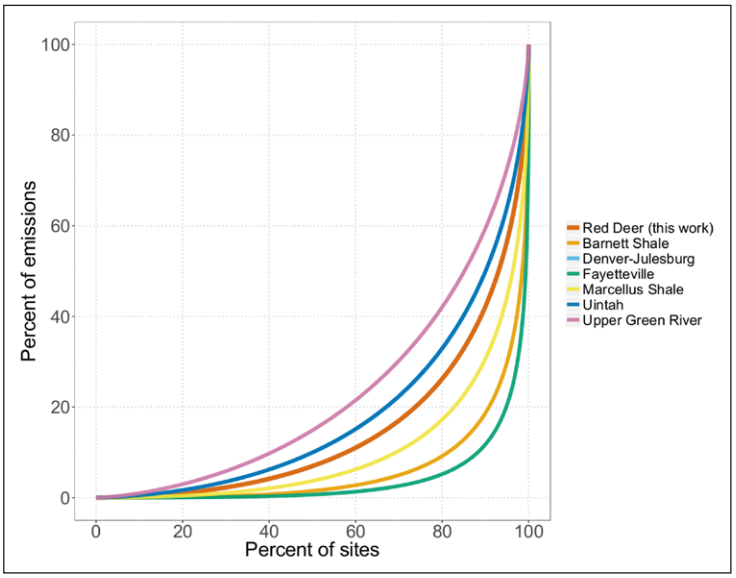

Figure 8: Lorenz curve for the different North American production regions where ground-based downwind measurements of oil and gas production sites have been reported (Rella et al., 2015; Zavala-Araiza, Lyon, et al., 2015; Robertson et al., 2017). Percent of emissions is shown as a function of percent of sites. In all cases, the emissions distributions are characterized by a disproportionate influence of high-emitting sites. The Red Deer region characterized in this work (red line) is more skewed than the Denver-Julesburg, Uintah (Uintah line on top of Denver-Julesburg line), and Upper Green river production regions. DOI: https://doi.org/10.1525/elementa.284.f8

be related to the different levels of skewedness, we want to underscore that the Red Deer production region seems to fit into a wider group of North American production regions where high-emitting sites are drivers of emissions.

We also look at the relationships between emissions and production parameters (**Figure 9**). When we compare Upper Green River and Red Deer, we see similar EFs (Upper Green River: 2.4 kg CH_4 h^{-1}, Red Deer: 2.2 kg CH_4 h^{-1}), but gas production and oil production are 25× and 20× higher than in Red Deer. This could be explained by the higher skewedness in the Red Deer emissions distributions (**Figure 8**, and Gini coefficient in **Figure 9**) – illustrating greater influence of high emitting sites.

As noted above, the median loss rate of 3.3% in Red Deer (**Figure 9**) should be used cautiously, since average gas production is significantly lower than in the other production regions analyzed to date (the much smaller denominator makes it very sensitive to small changes in emissions– particularly from oil production). Focusing specifically on the 19 sites classified as gas sites (within the 25 sites from the systematic sample), the mean loss rate was ~3% with a 95% confidence interval of 2–5% (calculated via a bootstrapping analysis). This high rate may be heavily impacted by the low production volume at gas wells in this region. However, this gas-site specific loss rate is potentially directly comparable to natural gas wells in other regions with similar production characteristics, and is indicative of the GHG-intensity of natural gas production in the Red Deer region.

Implications

Our work indicates that high-emitting sites in Red Deer disproportionately account for the majority of emissions. This finding is consistent with several studies in the US that report CH_4 emissions from oil and gas production sites. Using the definition proposed in Zavala-Araiza et al. (Zavala-Araiza et al., 2017), we hypothesize that a significant fraction of these high-emitting sites are super-emitters: sites with large unintended emissions related to abnormal process conditions (e.g., malfunctions, equipment issues). Zavala-Araiza et al. showed that emissions related to routine operating conditions were not enough to explain sources at high-emitting sites, thus the high-emitting sites are most likely related to abnormal process conditions. A similar conclusion was also reached by an infrared camera survey of 8,000 gas-producing sites across the US (Lyon et al., 2016). On-site, high-frequency measurements are needed to find the root cause of high-emitting sites, nonetheless, it is expected that – as observed in other North American production regions with skewed emission distributions – abnormal process conditions are responsible for high emitting sites in the Red Deer region.

When super-emitting sites are present, different sites may experience such abnormal conditions at different points in time (e.g., the same site will not always have the same malfunction, or an equipment issue could manifest at different sites at varying times). Thus mitigating emissions effectively requires frequent monitoring with the time between inspections short enough to minimize the duration of spatio-temporally dynamic super-emitting sites (Lyon et al., 2016; Lavoie et al., 2017).

In addition to the mitigation opportunity related to the super-emitters, a significant fraction of sites had detectable emissions. In other words, other sources of unreported emissions (e.g., pneumatic controllers, fugitive emissions) are likely causes of detected emissions at a large fraction of production sites; regulatory action

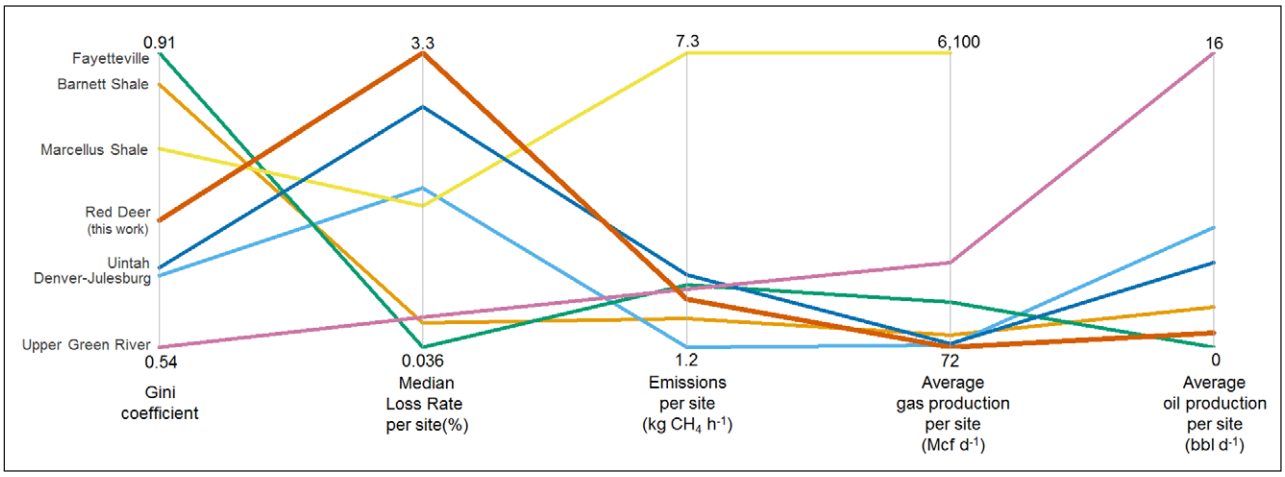

Figure 9: Parallel coordinates plot (Wegman, 1990) comparing emissions and production parameters for different North American production regions. For each production region, we plot each parameter on a parallel y-axis, with the range of values shown in the plot. The Gini coefficient represents a measure of disproportionality: the closer to one, the greater the influence from a small number of high-emitting sites (Collins et al., 2016; Zavala-Araiza et al., 2017). Proportional loss rate values represent the median loss rate from the emission distribution for each production region. Emissions represent the central EF for each production region. We also plot mean gas production and mean oil production for each production region (for the sampled populations). No oil production was reported for the Marcellus Shale production sites. DOI: https://doi.org/10.1525/elementa.284.f9

should address these sources through a combination of replacement of high-emitting equipment as well as comprehensive and more frequent leak detection and repair programs.

We also showed that emissions are related to age of sites as well as oil and gas production. When we add these relationships on top of the stochastic nature of super-emitters we end up with a complex landscape where it is hard to predict where emissions will appear. As a consequence, widespread inspection and control strategies are critical to reducing emissions until it is possible to accurately predict where and when emissions are likely to occur, something that should be possible once more data is available. With a probabilistic understanding of the sources of emissions they can be prophylactically avoided through routine maintenance and/or observation.

We acknowledge that the Red Deer production region might not be representative of other production regions in Alberta or Canada. However, this first characterization illustrates important similarities between production sites in North America. Future work should focus on collecting additional empirical observations at other regions where different geologic characteristics, operation practices, and age of sites might affect emission patterns.

Data Accessibility Statement

Site IDs, method, methane emission rates with 95% confidence interval, gas production, oil production, age, wells per site, reported emissions, and methane content in gas are uploaded as SM Dataset S1 in Microsoft Excel. xlsx format.

Supplemental Files

The supplemental files for this article can be found as follows:

- **File S1.** Measured production sites (xlsx). DOI: https://doi.org/10.1525/elementa.284.s1
- **Text S1-7.** Supplemental discussion (PDF). DOI: https://doi.org/10.1525/elementa.284.s2

Acknowledgement

We appreciate the assistance received from Gerald Palanca at Alberta Energy Regulator (AER) as well as Mike D'Antoni's support during the measurements. We are very grateful to Conner Daube and Jason Curry at Aerodyne Research, Inc.

Funding information

Funding for this work was provided by the generous supporters of the Environmental Defense Fund (EDF).

Competing interests

The authors declare no competing financial interest. DZA and MO work for Environmental Defense Fund (EDF), a non-profit organization funded by philanthropic contributions, which does not accept donations from the oil and gas industry in accordance with its corporate donations policy (https://www.edf.org/approach/partnerships/corporate-donation-policy).

Author contribution

- Contributed to conception and design: DZA, SCH, JRR, TIY, MRJ, DRT
- Performed measurements: SCH, JRR, TIY
- Contributed to analysis and interpretation of data: DZA, SCH, JRR, TIY, MRJ, DRT, MO, BK
- Drafted and/or revised the article: DZA, SCH, JRR, TIY, MRJ, DRT, MO, BK
- Approved the submitted version of the article: DZA, SCH, JRR, TIY, MRJ, DRT, MO, BK

References

AER 2016 Directive 060: Upstream petroleum industry flaring, incinerating, and venting. Calgary, AB, Canada.

Alberta Energy Regulator 2017 ST37. ST37: List of wells in Alberta monthly report. Available at: https://www.aer.ca/data-and-publications/statistical-reports/st37 Accessed 2017 Jun 23.

Alberta Government 2016 Reducing methane emissions. Available at: http://www.alberta.ca/climate-methane-emissions.aspx Accessed 2017 Jul 7.

Allen, DT, Pacsi, AP, Sullivan, DW, Zavala-Araiza, D, Harrison, M, Keen, K, Fraser, MP, Daniel Hill, A, Sawyer, RF and **Seinfeld, JH** 2015 Methane emissions from process equipment at natural gas production sites in the United States: pneumatic controllers. *Environ Sci Technol* **49**(1): 633–640. DOI: https://doi.org/10.1021/es5040156

Allen, DT, Sullivan, DW, Zavala-Araiza, D, Pacsi, AP, Harrison, M, Keen, K, Fraser, MP, Daniel Hill, A, Lamb, BK, Sawyer, RF, et al. 2015 Methane emissions from process equipment at natural gas production sites in the United States: liquid unloadings. *Environ Sci Technol* **49**(1): 641–648. DOI: https://doi.org/10.1021/es504016r

Allen, DT, Torres, VM, Thomas, J, Sullivan, DW, Harrison, M, Hendler, A, Herndon, SC, Kolb, CE, Fraser, MP, Hill, AD, et al. 2013 Measurements of methane emissions at natural gas production sites in the United States. *Proc Natl Acad Sci* **110**(44): 17768–17773. DOI: https://doi.org/10.1073/pnas.1304880110

Atherton, E, Risk, D, Fougère, C, Lavoie, M, Marshall, A, Werring, J, Williams, JP and **Minions, C** 2017 Mobile measurement of methane emissions from natural gas developments in Northeastern British Columbia, Canada. *Atmos Chem Phys* **17**(20): 12405–12420. DOI: https://doi.org/10.5194/acp-17-12405-2017

Baihly, JD, Altman, RM, Malpani, R and **Luo, F** 2010 Shale gas production decline trend comparison over time and basins. SPE annual technical conference and exhibition. Society of Petroleum Engineers. Available at: https://www.onepetro.org/conference-paper/SPE-135555-MS Accessed 2017 Jul 10.

Bousquet, P, Ciais, P, Miller, JB, Dlugokencky, EJ, Hauglustaine, DA, Prigent, C, Van der Werf, GR, Peylin, P, Brunke, E-G, Carouge, C, et al. 2006 Contribution of anthropogenic and natural sources to atmospheric methane variability. *Nature* **443**(7110): 439–443. DOI: https://doi.org/10.1038/nature05132

Brandt, AR, Heath, GA and **Cooley, D** 2016 Methane leaks from natural gas systems follow extreme distributions. *Environ Sci Technol* **50**(22): 12512–12520. DOI: https://doi.org/10.1021/acs.est.6b04303

Brandt, AR, Heath, GA, Kort, EA, O'Sullivan, F, Petron, G, Jordaan, SM, Tans, P, Wilcox, J, Gopstein, AM, Arent, D, et al. 2014 Methane leaks from North American natural gas systems. *Science* **343**(6172): 733–735. DOI: https://doi.org/10.1126/science.1247045

Brantley, HL, Thoma, ED, Squier, WC, Guven, BB and **Lyon, D** 2014 Assessment of methane emissions from oil and gas production pads using mobile measurements. *Environ Sci Technol* **48**(24): 14508–14515. DOI: https://doi.org/10.1021/es503070q

Clearstone Engineering Ltd 2014 UOG Emissions inventory volume 3: UOG emissions inventory methodology manual. Environment Canada.

Climate & Clean Air Coalition 2016 Nov 15 Coalition ministers pledge to reduce the impacts of methane and black carbon on climate and health. Available at: http://ccacoalition.org/en/news/coalition-ministers-pledge-reduce-impacts-methane-and-black-carbon-climate-and-health Accessed 2017 Jul 7.

Collins, MB, Munoz, I and **JaJa, J** 2016 Linking "toxic outliers" to environmental justice communities. *Environ Res Lett* **11**(1): 015004. DOI: https://doi.org/10.1088/1748-9326/11/1/015004

DI Desktop 2017 Drillinginfo. Austin, TX: Drillinginfo. Available at: http://www.didesktop.com/ Accessed 2017 Aug 1.

Efron, B and **Tibshirani, RJ** 1993 An Introduction to the bootstrap: monographs on statistics and applied probability **57**. *N Y Lond Chapman HallCRC*, in press.

Environment and Climate Change Canada 2016 National inventory report 1990–2014: greenhouse gas sources and sinks in Canada. Available at: http://publications.gc.ca/collections/collection_2016/eccc/En81-4-1-2014-eng.pdf Accessed 2017 Jul 7.

Environment and Climate Change Canada 2017a May 25 Canada to reduce emissions from oil and gas industry. gcnws. Available at: https://www.canada.ca/en/environment-climate-change/news/2017/05/canada_to_reduceemissionsfromoilandgasindustry.html Accessed 2017 Jul 7.

Environment and Climate Change Canada 2017b May 27 Canada Gazette – Regulations respecting reduction in the release of methane and certain volatile organic compounds (upstream oil and gas sector). Available at: http://www.gazette.gc.ca/rp-pr/p1/2017/2017-05-27/html/reg1-eng.php Accessed 2017 Jul 7.

Herndon, SC, Jayne, JT, Zahniser, MS, Worsnop, DR, Knighton, B, Alwine, E, Lamb, BK, Zavala, M, Nelson, DD, McManus, JB, et al. 2005 Characterization of urban pollutant emission fluxes and ambient concentration distributions using a mobile laboratory with rapid response instrumentation. *Faraday Discuss* **130**: 327. DOI: https://doi.org/10.1039/b500411j

Höglund-Isaksson, L 2017 Bottom-up simulations of methane and ethane emissions from global oil and gas systems 1980 to 2012. *Environ Res Lett* **12**(2): 024007. DOI: https://doi.org/10.1088/1748-9326/aa583e

Johnson, MR, Tyner, DR, Conley, S, Schwietzke, S and **Zavala-Araiza, D** 2017 Comparisons of airborne measurements and inventory estimates of methane emissions in the Alberta upstream oil and gas sector. *Environ Sci Technol* **51**(21). DOI: https://doi.org/10.1021/acs.est.7b03525

Knighton, WB, Herndon, SC, Franklin, JF, Wood, EC, Wormhoudt, J, Brooks, W, Fortner, EC and **Allen, DT** 2012 Direct measurement of volatile organic compound emissions from industrial flares using real-time online techniques: proton transfer reaction mass spectrometry and tunable infrared laser differential absorption spectroscopy. *Ind Eng Chem Res* **51**(39): 12674–12684. DOI: https://doi.org/10.1021/ie202695v

Kolb, CE, Herndon, SC, McManus, JB, Shorter, JH, Zahniser, MS, Nelson, DD, Jayne, JT, Canagaratna, MR and **Worsnop, DR** 2004 Mobile laboratory with rapid response instruments for real-time measurements of urban and regional trace gas and particulate distributions and emission source characteristics. *Environ Sci Technol* **38**(21): 5694–5703. DOI: https://doi.org/10.1021/es030718p

Lamb, BK, Edburg, SL, Ferrara, TW, Howard, T, Harrison, MR, Kolb, CE, Townsend-Small, A, Dyck, W, Possolo, A and **Whetstone, JR** 2015 Direct measurements show decreasing methane emissions from natural gas local distribution systems in the United States. *Environ Sci Technol* **49**(8): 5161–5169. DOI: https://doi.org/10.1021/es505116p

Lamb, BK, McManus, JB, Shorter, JH, Kolb, CE, Mosher, B, Harriss, RC, Allwine, E, Blaha, D, Howard, T, Guenther, A, et al. 1995 Development of atmospheric tracer methods to measure methane emissions from natural gas facilities and urban areas. *Environ Sci Technol* **29**(6): 1468–1479. DOI: https://doi.org/10.1021/es00006a007

Lan, X, Talbot, R, Laine, P and **Torres, A** 2015 Characterizing fugitive methane emissions in the Barnett Shale area using a mobile laboratory. *Environ Sci Technol* **49**(13): 8139–8146. DOI: https://doi.org/10.1021/es5063055

Lavoie, TN, Shepson, PB, Cambaliza, MOL, Stirm, BH, Conley, S, Mehrotra, S, Faloona, IC and **Lyon, D** 2017 Spatiotemporal variability of methane emissions at oil and natural gas operations in the Eagle Ford Basin. *Environ Sci Technol* **51**(14): 8001–8009. DOI: https://doi.org/10.1021/acs.est.7b00814

Lyon, DR, Alvarez, RA, Zavala-Araiza, D, Brandt, AR, Jackson, RB and **Hamburg, SP** 2016 Apr 5 Aerial surveys of elevated hydrocarbon emissions from oil and gas production sites. *Environ Sci Technol*, in press. DOI: https://doi.org/10.1021/acs.est.6b00705

Marchese, AJ, Vaughn, TL, Zimmerle, DJ, Martinez, DM, Williams, LL, Robinson, AL, Mitchell, AL, Subramanian, R, Tkacik, DS, Roscioli, JR, et al. 2015 Aug 18 Methane emissions from United States natural gas gathering and processing. *Environ Sci Technol*, in press. DOI: https://doi.org/10.1021/acs.est.5b02275

McManus, JB, Zahniser, MS, Nelson, DD, Shorter, JH, Herndon, SC, Jervis, D, Agnese, M, McGovern, R, Yacovitch, TI and **Roscioli, JR** 2015 Recent progress in laser-based trace gas instruments: performance and noise analysis. *Appl Phys B* **119**(1): 203–218. DOI: https://doi.org/10.1007/s00340-015-6033-0

Mexico: Presidencia de la Republica 2016 Declaración de líderes de América del Norte sobre la alianza del clima, energía limpia y medio ambiente. gob.mx. Available at: http://www.gob.mx/presidencia/documentos/declaracion-de-lideres-de-america-del-norte-sobre-la-alianza-del-clima-energia-limpia-y-medio-ambiente Accessed 2017 Jul 7.

Mitchell, AL, Tkacik, DS, Roscioli, JR, Herndon, SC, Yacovitch, TI, Martinez, DM, Vaughn, TL, Williams, LL, Sullivan, MR, Floerchinger, C, et al. 2015 Measurements of methane emissions from natural gas gathering facilities and processing plants: measurement results. *Environ Sci Technol* **49**(5): 3219–3227. DOI: https://doi.org/10.1021/es5052809

Omara, M, Sullivan, MR, Li, X, Subramanian, R, Robinson, AL and **Presto, AA** 2016 Methane emissions from conventional and unconventional natural gas production sites in the Marcellus Shale Basin. *Environ Sci Technol* **50**(4): 2099–2107. DOI: https://doi.org/10.1021/acs.est.5b05503

Rella, CW, Tsai, TR, Botkin, CG, Crosson, ER and **Steele, D** 2015 Measuring emissions from oil and natural gas well pads using the mobile flux plane technique. *Environ Sci Technol* **49**(7): 4742–4748. DOI: https://doi.org/10.1021/acs.est.5b00099

Robertson, AM, Edie, R, Snare, D, Soltis, J, Field, RA, Burkhart, MD, Bell, CS, Zimmerle, D and **Murphy, SM** 2017 Jun 19 Variation in methane emission rates from well pads in four oil and gas basins with contrasting production volumes and compositions. *Environ Sci Technol*, in press. DOI: https://doi.org/10.1021/acs.est.7b00571

Roscioli, JR, Yacovitch, TI, Floerchinger, C, Mitchell, AL, Tkacik, DS, Subramanian, R, Martinez, DM, Vaughn, TL, Williams, L, Zimmerle, D, et al. 2015 Measurements of methane emissions from natural gas gathering facilities and processing plants: measurement methods. *Atmospheric Meas Tech* **8**(5): 2017–2035. DOI: https://doi.org/10.5194/amt-8-2017-2015

Saunois, M, Bousquet, P, Poulter, B, Peregon, A, Ciais, P, Canadell, JG, Dlugokencky, EJ, Etiope, G, Bastviken, D, Houweling, S, et al. 2016 The global methane budget 2000–2012. *Earth Syst Sci Data* **8**(2): 697. DOI: https://doi.org/10.5194/essd-8-697-2016

Shoemaker, JK, Schrag, DP, Molina, MJ and **Ramanathan, V** 2013 What role for short-lived climate pollutants in mitigation policy? *Science* **342**(6164): 1323–1324. DOI: https://doi.org/10.1126/science.1240162

Thoma, ED, Squier, BC, Olson, D, Gehrke, G, Eisele, AP, Miller, M, DeWees, JM, Segall, RR, Amin, MS

and **Modrak, MT** 2012 Assessment of methane and VOC emissions from select oil and gas production operations using remote measurements, interim report on survey studies in CO, TX and WY. 2012. AWMA Symposium on Air Quality Measurement Methods and Technology; Durham, North Carolina.

Turner, BD 1994 Workbook of atmospheric dispersion modeling: an introduction to dispersion modeling. *Boca Raton FL CRC*, in press.

US EPA 2014 Other test method (OTM) 33 and 33A geospatial measurement of air pollution – remote emissions quantification – direct assessment (GMAP-REQ-DA). Available at: https://www3.epa.gov/ttnemc01/prelim/otm33a.pdf.

US EPA 2016 May 11 EPA releases first-ever standards to cut methane emissions from the oil and gas sector. US EPA. Available at: https://www.epa.gov/newsreleases/epa-releases-first-ever-standards-cut-methane-emissions-oil-and-gas-sector Accessed 2017 Jul 7.

Wegman, EJ 1990 Hyperdimensional data analysis using parallel coordinates. *J Am Stat Assoc* **85**(411): 664–675. DOI: https://doi.org/10.1080/01621459.1990.10474926

Yacovitch, TI, Daube, C, Vaughn, TL, Bell, CS, Roscioli, JR, Knighton, WB, et al. 2017 Natural gas facility methane emissions: measurements by tracer flux ratio in two US natural gas producing basins. *Elem Sci Anth* **5**: 69. DOI: https://doi.org/10.1525/elementa.251

Yacovitch, TI, Herndon, SC, Pétron, G, Kofler, J, Lyon, D, Zahniser, MS and **Kolb, CE** 2015 Mobile laboratory observations of methane emissions in the Barnett Shale Region. *Environ Sci Technol* **49**(13): 7889–7895. DOI: https://doi.org/10.1021/es506352j

Yacovitch, TI, Herndon, SC, Roscioli, JR, Floerchinger, C, McGovern, RM, Agnese, M, Pétron, G, Kofler, J, Sweeney, C, Karion, A, et al. 2014 Demonstration of an ethane spectrometer for methane source identification. *Environ Sci Technol* **48**(14): 8028–8034. DOI: https://doi.org/10.1021/es501475q

Zavala-Araiza, D, Allen, DT, Harrison, M, George, FC and **Jersey, GR** 2015 Allocating methane emissions to natural gas and oil production from shale formations. *ACS Sustain Chem Eng* **3**(3): 492–498. DOI: https://doi.org/10.1021/sc500730x

Zavala-Araiza, D, Alvarez, RA, Lyon, DR, Allen, DT, Marchese, AJ, Zimmerle, DJ and **Hamburg, SP** 2017 Super-emitters in natural gas infrastructure are caused by abnormal process conditions. *Nat Commun* **8**: 14012. DOI: https://doi.org/10.1038/ncomms14012

Zavala-Araiza, D, Lyon, D, Alvarez, RA, Palacios, V, Harriss, R, Lan, X, Talbot, R and **Hamburg, SP** 2015 Toward a functional definition of methane super-emitters: application to natural gas production sites. *Environ Sci Technol* **49**(13): 8167–8174. DOI: https://doi.org/10.1021/acs.est.5b00133

Zavala-Araiza, D, Lyon, DR, Alvarez, RA, Davis, KJ, Harriss, R, Herndon, SC, Karion, A, Kort, EA, Lamb, BK, Lan, X, et al. 2015 Reconciling divergent estimates of oil and gas methane emissions. *Proc Natl Acad Sci* **112**(51): 15597–15602. DOI: https://doi.org/10.1073/pnas.1522126112

Zimmerle, DJ, Williams, LL, Vaughn, TL, Quinn, C, Subramanian, R, Duggan, GP, Willson, B, Opsomer, JD, Marchese, AJ, Martinez, DM, et al. 2015 Methane Emissions from the natural gas transmission and storage system in the United States. *Environ Sci Technol* **49**(15): 9374–9383. DOI: https://doi.org/10.1021/acs.est.5b01669

How to cite this article: Zavala-Araiza, D, Herndon, SC, Roscioli, JR, Yacovitch, TI, Johnson, MR, Tyner, DR, Omara, M and Knighton, B 2018 Methane emissions from oil and gas production sites in Alberta, Canada. *Elem Sci Anth,* 6: 27. DOI: https://doi.org/10.1525/elementa.284

Domain Editor-in-Chief: Detlev Helmig, Fellow and Associate Research Professor, University of Colorado Boulder, US

Guest Editor: Stefan Schwietzke, National Oceanic and Atmospheric Administration and University of Colorado, US

Knowledge Domain: Atmospheric Science

Part of an *Elementa* Special Forum: Oil and Natural Gas Development: Air Quality, Climate Science, and Policy

Submitted: 18 October 2017 **Accepted:** 19 February 2018 **Published:** 22 March 2018

ELEMENTA Science of the Anthropocene

Elem Sci Anth is a peer-reviewed open access journal published by University of California Press.

OPEN ACCESS